

# Buckling and Post-buckling Analysis of FG-CNTRC Beams: An Exact Closed Form Solution

H. Shafiei<sup>1\*</sup> and A.R. Setoodeh<sup>2</sup>

1,2. Department of Mechanical and Aerospace Engineering, Shiraz University of Technology

\*Postal Code: 71555, Shiraz, IRAN

[h.shafiei@sutech.ac.ir](mailto:h.shafiei@sutech.ac.ir)

*The present work derives the exact analytical solutions for buckling and post-buckling analysis of nano-composite beams reinforced by single-walled carbon nanotubes (SWCNTs) based on the Euler-Bernoulli beam theory and principle of virtual work. The reinforcements are considered to be aligned in the polymeric matrix either uniformly distributed (UD) or functionally graded (FG) distributed through the thickness direction of the beam. In FG beams, material properties vary gradually along the thickness direction. The effective material properties of the nano-composite beam are predicted based on the extended rule of mixture. Also, by applying von Kármán assumptions, the geometric nonlinearities are taken into consideration. The developed governing equations are solved by utilizing analytical methods and exact closed form solutions for buckling and post-buckling loads of functionally graded carbon nanotube-reinforced composite (FG-CNTRC) beam with different boundary conditions are obtained. By comparing the present post-buckling load results with the ones reported in the literature, the accuracy and reliability of the current method are demonstrated. Eventually, the numerical results are provided and the effects of CNTs distribution, CNTs volume fraction, slenderness ratio, maximum deflection of the beam and boundary conditions on the post-buckling characteristics of the CNTRC beam are discussed.*

**Keywords:** Post-buckling analysis, Nano-composite beams, Functionally graded materials, Exact solution

## Introduction

By the improvement of science and technology, new advanced nanomaterials have been introduced and due to their significant electrical, mechanical and thermal properties, they have been employed in different fields of science and industry. Carbon nanotubes (CNTs) are one of these novel materials which have wide potential applications such as reinforcements in composite materials [1-5]. Subsequently, carbon nanotube reinforced composites (CNTRCs) have become an interesting field of study and their mechanical properties have been examined by several researchers to find their

maximum efficiency [6-9]. These studies confirm that CNTRCs are suitable materials to be used in real structural elements such as plates and beams. Accordingly, the studies on the mechanical behavior of such structures have rapidly increased [10-15]. Ke et al. [16] employed Ritz method and a direct iterative technique to discuss nonlinear free vibration of FG-CNTRC Timoshenko beams. They showed that an increase in CNTs volume fraction leads to higher linear and nonlinear natural frequencies. Zhang et al. [17] conducted a study to analyze the buckling behavior of FG-CNTRC thick skew plates based on the first-order shear deformation theory. Nonlinear free vibration of FG-CNTRC plates was investigated by Setoodeh et al. [18] utilizing classical plate theory together with differential quadrature method.

---

1. M. Sc. (Corresponding Author)  
2. Professor

Applying a higher order shear deformation beam theory, Shen et al. [19] examined vibration of a thermally post-buckled CNTRC beam on an elastic foundation. It was found that FG reinforcement has a significant effect on the vibrational parameters of post-buckled CNTRC beams.

Due to high ratio of length to thickness in most of the beams/nano-beams, the buckling and post-buckling behavior of CNTRC beams are of great importance to the scientists. For instance, Yas and Samadi [20] considered various distributions of CNTs in the matrix and studied buckling and free vibration of FG-CNTRC Timoshenko beams resting on an elastic foundation. Wu et al. [21] investigated the post-buckling behavior of a geometrically imperfect FG-CNTRC beam with different imperfection modes and revealed that post-buckling behavior is extremely sensitive to the imperfection amplitude. Based on the Timoshenko beam theory together with the differential quadrature method, Wu et al. [22] analyzed the thermal buckling and post-buckling of FG-CNTRC beams. A nonprobabilistic approach was employed by Poursmaeeli et al. [23] to discuss the buckling of FG-CNTRC beams in the presence of the material and geometrical uncertainties.

According to the literature, buckling and post-buckling behavior of CNTRC beams have been studied by some researchers, but to the best of the authors' knowledge, no exact closed form solutions are reported. The purpose of this paper is to develop exact analytical expressions for buckling and post-buckling analysis of an axially loaded nano-composite beam reinforced by SWCNTs. The extended rule of mixture is utilized to determine the effective material properties of FG-CNTRC beam. The governing equation is derived using Euler-Bernoulli beam theory and von Kármán assumptions are taken into account to apply the geometric nonlinearities. The numerical results for fully clamped (CC) as well as simply supported (SS) FG-CNTRC beams are presented to evaluate the influences of different parameters such as CNTs volume fraction, CNTs distribution in the matrix, slenderness ratio, and dimensionless amplitude on the post-buckling characteristics of the nano-composite beams.

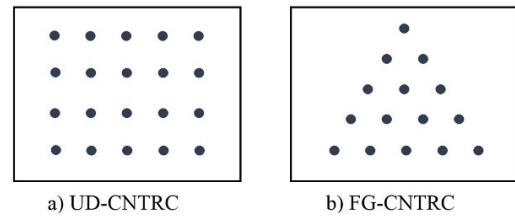


Figure 1. CNTs distribution in the matrix

### Effective Material Properties of FG-CNTRC Beam

The CNTRC beam is made of SWCNTs embedded in the isotropic matrix with the distribution patterns shown in Fig. 1. According to the extended rule of mixture, the effective material properties of a CNTRC can be indicated as [16]:

$$E_{11} = \eta_1 V^{cnt} E_{11}^{cnt} + V_m E_m \tag{1a}$$

$$\frac{\eta_2}{E_{22}} = \frac{V^{cnt}}{E_{22}^{cnt}} + \frac{V_m}{E_m} \tag{1b}$$

$$\frac{\eta_3}{G_{12}} = \frac{V^{cnt}}{G_{12}^{cnt}} + \frac{V_m}{G_m} \tag{1c}$$

$$\nu = V^{cnt} \nu^{cnt} + V_m \nu_m \tag{1d}$$

$$\rho = V^{cnt} \rho^{cnt} + V_m \rho_m \tag{1e}$$

Where  $E_{11}^{cnt}$ ,  $E_{22}^{cnt}$  and  $G_{12}^{cnt}$  are Young's modulus and shear modulus of the CNTs, respectively.  $E_m$  and  $G_m$  stand for the corresponding material properties of the isotropic matrix. Also,  $\nu$  is the Poisson's ratio and  $\rho$  denotes the mass density.  $\eta_i$  ( $i=1,2,3$ ) are the CNTs efficiency parameters accounting for the size-dependent material properties and will be assessed later by equalizing the elastic moduli solutions estimated from molecular dynamics (MD) simulations [6] and those obtained from the extended rule of mixture.  $V_m$  and  $V^{cnt}$  refer to the volume fraction of the matrix and CNTs while  $V_m + V^{cnt} = 1$ . For the distribution patterns of CNTs in the matrix, the following relations are considered:

$$\begin{aligned} \text{UD: } V^{cnt} &= V_*^{cnt} \\ \text{FG: } V^{cnt} &= \left(1 + \frac{2z}{h}\right) V_*^{cnt} \end{aligned} \tag{2}$$

where

$$V_*^{cnt} = \frac{A^{cnt}}{A^{cnt} + \left(\frac{\rho^{cnt}}{\rho_m}\right)(1 - A^{cnt})} \tag{3}$$

in which  $A^{cnt}$  is the mass fraction of CNTs.

**Derivation of Governing Equation**

To obtain the equation of motion of the beam, the Cartesian coordinate system is considered on the central axis of the beam with the  $x$ ,  $y$  and  $z$  axes along the length, width, and thickness of the beam, respectively. Based on the Euler-Bernoulli beam theory, the displacement of an arbitrary point of the beam in the  $x$  and  $z$  directions can be described as:

$$\bar{U}(x, z) = U(x) - z \frac{dW(x)}{dx}, \quad \bar{W}(x, z) = W(x) \quad (4)$$

where  $U$  and  $W$  refer to the axial and transverse displacements at the mid-plane of the beam, respectively. It should be mentioned that since the buckling and post-buckling analysis are time independent, the time variable is omitted. Using von Kármán assumptions, the normal stress  $\sigma_{xx}$  takes the following form:

$$\sigma_{xx} = Q_{11}(z) \left[ \frac{dU}{dx} - z \frac{d^2W}{dx^2} + \frac{1}{2} \left( \frac{dW}{dx} \right)^2 \right] \quad (5)$$

in which

$$Q_{11} = \frac{E_{11}(z)}{1 - \nu^2(z)} \quad (6)$$

According to the principle of virtual work, one can write:

$$\delta(U_e - W_{ex}) = 0 \quad (7)$$

where  $\delta$  represents the variational symbol. Also,  $U_e$  is the strain energy of the beam, and  $W_{ex}$  denotes the work done by the external axial force. Substituting the relations of  $U_e$  and  $W_{ex}$  in the principle of virtual work, employing integration by parts and then, setting the coefficients of  $\delta U$  and  $\delta W$  equal to zero, the governing equations of the CNTRC beam of the length  $l$ , width  $b$ , and thickness  $h$ , are derived as:

$$\frac{dN}{dx} = 0 \quad (8)$$

$$\frac{d^2M}{dx^2} + \frac{d}{dx} \left( N \frac{dW}{dx} \right) - f \frac{d^2W}{dx^2} = 0 \quad (9)$$

where  $f$  is the axial force, and  $N$  and  $M$  represent respectively the force and bending moment resultants, as:

$$N = A_{11} \left[ \frac{dU}{dx} + \frac{1}{2} \left( \frac{dW}{dx} \right)^2 \right] - B_{11} \frac{d^2W}{dx^2} \quad (10)$$

$$M = B_{11} \left[ \frac{dU}{dx} + \frac{1}{2} \left( \frac{dW}{dx} \right)^2 \right] - D_{11} \frac{d^2W}{dx^2} \quad (11)$$

in which

$$\{A_{11}, B_{11}, D_{11}\} = \int_{-\frac{h}{2}}^{\frac{h}{2}} Q_{11}(z) \{1, z, z^2\} dz \quad (12)$$

Eq. (8) indicates that  $N = \text{constant} = N_0$ . Therefore, according to immovable end supports, integration from (10) yields:

$$N_0 = \frac{A_{11}}{l} \int_0^l \left[ \frac{1}{2} \left( \frac{dW}{dx} \right)^2 - \frac{B_{11}}{A_{11}} \frac{d^2W}{dx^2} \right] dx \quad (13)$$

Also, the bending resultant is restated as:

$$M = \frac{B_{11}}{A_{11}} \left[ N_0 + B_{11} \frac{d^2W}{dx^2} \right] - D_{11} \frac{d^2W}{dx^2} \quad (14)$$

Thus, the governing equation of post-buckling of the FG-CNTRC beam is reduced to:

$$\left( \frac{B_{11}^2}{A_{11}} - D_{11} \right) \frac{d^4W}{dx^4} + (N_0 - f) \frac{d^2W}{dx^2} = 0 \quad (15)$$

Introducing the following dimensionless quantities:

$$\zeta = \frac{x}{l}, \quad w = \frac{W}{h}, \quad \eta = \frac{h}{l}, \quad (16)$$

$$(a_{11}, b_{11}, d_{11}) = \left( \frac{A_{11}}{A_{110}}, \frac{B_{11}}{A_{110}h}, \frac{D_{11}}{A_{110}h^2} \right)$$

where  $A_{110}$  is the value of  $A_{11}$  of a homogeneous beam made of matrix material, the dimensionless governing equation of the CNTRC beam takes the form of:

$$d_0 \eta^2 \frac{d^4w}{d\zeta^4} + (\bar{N}_0 - F) \frac{d^2w}{d\zeta^2} = 0 \quad (17)$$

in which  $F$  denotes the dimensionless axial force and:

$$F = \frac{f}{A_{110}}, \quad d_0 = \frac{b_{11}^2}{a_{11}} - d_{11} \quad (18)$$

$$\bar{N}_0 = a_{11} \eta^2 \int_0^1 \left[ \frac{1}{2} \left( \frac{dw}{d\zeta} \right)^2 - \frac{b_{11}}{a_{11}} \frac{d^2w}{d\zeta^2} \right] d\zeta$$

**Exact Solutions**

For simplification, the governing equation is rewritten as:

$$\frac{d^4w}{d\zeta^4} + \beta^2 \frac{d^2w}{d\zeta^2} = 0 \quad (19)$$

where  $\beta^2$  is a constant defined as:

$$\beta^2 = \frac{\bar{N}_0 - F}{d_0 \eta^2} \quad (20)$$

Eq. (19) is a fourth-order differential equation that has a general solution in the form of:

$$w(\zeta) = a_1 \sin(\beta \zeta) + a_2 \cos(\beta \zeta) + a_3 \zeta + a_4 \quad (21)$$

in which  $a_j(j=1,2,3,4)$  are unknown constants to be determined by satisfying the following boundary conditions for SS and CC beams:

SS beam:  $w(0) = w(1) = 0$ ,

$$\frac{d^2 w(0)}{d\zeta^2} = \frac{d^2 w(1)}{d\zeta^2} = 0 \quad (22)$$

CC beam:  $w(0) = w(1) = 0$ ,

$$\frac{dw(0)}{d\zeta} = \frac{dw(1)}{d\zeta} = 0 \quad (23)$$

Substituting Eq. (21) into Eqs. (22) and (23) leads to the characteristic equations for, respectively, SS and CC boundary conditions as:

$$\sin \beta = 0 \quad (24)$$

$$2 - 2\cos \beta - \beta \sin \beta = 0 \quad (25)$$

The first three values of  $\beta$  for SS beams are found to be  $\pi$ ,  $2\pi$  and  $3\pi$ . Also, the corresponding values for CC beams are calculated as  $2\pi$ ,  $2.8606\pi$ ,  $4\pi$ . The general closed form solution of the buckling mode shape of a CNTRC beam can be expressed as  $w(\zeta) = \gamma_n w_{max} \psi_n(\zeta)$ . One notes that  $n$  denotes the mode number and  $\gamma_n$  is a constant that is determined according to the maximum displacement of the beam which in the first mode is  $\gamma_1 = 1$  for SS beams and  $\gamma_1 = 1/2$  for CC beams. Thus, based on the boundary conditions, the function  $\psi_n$  is respectively calculated for SS and CC FG-CNTRC beams as:

$$\psi_n = \sin(\beta_n \zeta) \quad (26)$$

$$\psi_n = 1 - \frac{\beta_n - \beta_n \cos \beta_n}{\beta_n - \sin \beta_n} \zeta - \cos(\beta_n \zeta) + \frac{1 - \cos \beta_n}{\beta_n - \sin \beta_n} \sin(\beta_n \zeta) \quad (27)$$

In view of Eqs. (20), (26) and (27), the maximum dimensionless post-buckling amplitude of SS and CC nano-composite beams can be found by solving the following equation:

$$\theta_1 w_{max}^2 + \theta_2 w_{max} + \theta_3 = 0 \quad (28)$$

Where

Also, the dimensionless critical buckling load of the CNTRC beam associated with the different boundary conditions can be evaluated by setting  $w_{max} = 0$ .

$$\begin{aligned} \theta_1 &= \frac{a_{11} \gamma_n^2 \eta^2}{2} \int_0^1 \left( \frac{d\psi_n}{d\zeta} \right)^2 d\zeta, \\ \theta_2 &= -b_{11} \gamma_n \eta^2 \int_0^1 \frac{d^2 \psi_n}{d\zeta^2} d\zeta, \\ \theta_3 &= -(F + d_0 \eta^2 \beta^2) \end{aligned} \quad (29)$$

### Results and Discussions

In this section, a parametric study is conducted to show the effects of different variables on the post-buckling characteristics of FG-CNTRC beams. Also, the present solutions are compared with the results available from the literature to demonstrate the correctness of the current approach. The selected reinforcements are the armchair (10,10) SWCNTs aligned in a matrix made of poly methyl methacrylate (PMMA). The material properties of matrix and reinforcements are, respectively,  $\nu_m = 0.3$ ,  $\rho_m = 1190 \text{ kg/m}^3$ ,  $E_m = 2.5 \text{ GPa}$ ,  $\nu^{cnt} = 0.19$ ,  $E_{11}^{cnt} = 600 \text{ GPa}$ , and  $\rho^{cnt} = 1400 \text{ kg/m}^3$  [16]. By matching the CNTRC's Young's modulus evaluated from the extended rule of mixture with the ones predicted from MD simulations [6], The CNTs efficiency parameters are calculated as  $\eta_1 = 1.2833$  and  $\eta_2 = 1.0556$  for  $V_*^{cnt} = 0.12$ ,  $\eta_1 = 1.3414$  and  $\eta_2 = 1.7101$  for  $V_*^{cnt} = 0.17$ , and  $\eta_1 = 1.3238$  and  $\eta_2 = 1.7380$  for  $V_*^{cnt} = 0.28$  [16]. Moreover, it is assumed that  $\eta_2 = \eta_3$ . Unless otherwise indicated, all of the results are obtained using the slenderness ratio of  $l/h = 30$ .

Table 1 shows the comparison between the predicted dimensional buckling loads ( $F_l$ ) and those given by Emam and Nayfeh [24] for graphite-epoxy laminated composite beams. The first three buckling loads are presented for a laminated composite beam of the length  $l = 0.25 \text{ m}$ , width  $b = 0.01 \text{ m}$  and height  $h = 0.001 \text{ m}$  with two different lay-ups subjected to different boundary conditions. As it is seen, the results agree very well.

Fig. 2 plots the static bifurcation diagrams of CC and SS SWCNTs with material properties of  $E = 1 \text{ TPa}$ ,  $\nu = 0.19$ , and  $l = 10 \text{ nm}$ . The curves are compared with the results presented by Setoodeh et al. [25]. They assumed the CNTs as isotropic beams and used Eringen's nonlocal theory to apply the size-dependent effects. Their results for

SWCNTs while the scale parameter  $e_0a=0$  is utilized in this study. It can be seen that the curves exactly coincide with each other for both CC and SS boundary conditions.

One can note that  $P_{nl}$  is a nondimensional post-buckling load with the dimensionless relation of  $P_{nl}=f l^2/EI$ , and  $r = \sqrt{I/A}$ , where  $I$  and  $A$  are area moment of inertia and cross-section area of the beam, respectively. Also, nondimensional buckled deflection ( $W/r$ ) is calculated at one-fourth of the SWCNTs length.

Furthermore, analytical expressions for buckling mode shapes of a composite beam from other references [26,27] are considered and the values of buckling load ratios ( $F_{nl}/F_l$ ) of SS and CC FG-CNTRC beams with  $V_*^{cnt}=0.12$  are obtained. In Table 2, the solutions are compared with the results calculated using the mode shapes presented in this study and again, a good agreement is achieved.

**Table 1.** First three buckling loads ( $F_l$ ) for SS and CC laminated composite beams

	Unidirectional		$(0^\circ 90^\circ 90^\circ)_s$	
	Present	Ref. [24]	Present	Ref. [24]
<b>SS</b>				
$F_1$	20.4958	20.4956	14.8969	14.8969
$F_2$	81.9831	81.9823	59.5878	59.5876
$F_3$	181.4620	181.4600	134.0725	134.0720
<b>CC</b>				
$F_1$	81.9831	81.9823	59.5878	59.5876
$F_2$	167.7176	167.7150	121.9022	121.9010
$F_3$	327.9324	327.9290	238.3512	238.3500

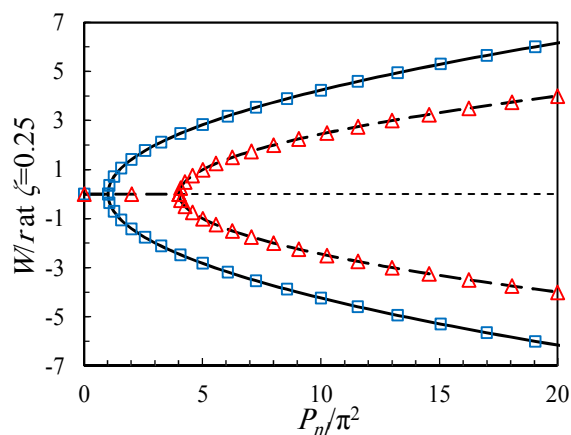


**Figure 2.** Static bifurcation diagrams for buckled configuration of SWCNTs (SS-Setoodeh et al. [25], SS-Present, CC-Setoodeh et al. [25], CC-Present)

**Table 2.** Buckling load ratios ( $F_{nl}/F_l$ ) for SS and CC FG-CNTRC beams

$w_{max}$	Present	Fallah and Aghdam [26]	Gupta et al. [27]
<b>SS</b>			
0.5	2.9927	2.9927	2.9927
1	7.1732	7.1732	7.1732
2	22.0977	22.0977	22.0977
3	45.7735	45.7735	45.7735
<b>CC</b>			
0.5	1.2735	1.2714	1.2735
1	2.0939	2.0814	2.0939
2	5.3756	5.3255	5.3756
3	10.8452	10.7324	10.8451

The effect of volume fraction on the dimensionless post-buckling loads versus dimensionless maximum amplitudes of UD-CNTRC and FG-CNTRC beams is shown in Fig. 3. The results demonstrate that dimensionless post-buckling loads increase with the raise in volume fraction. In other words, increasing the amount of CNTs in the matrix enhances the stiffness of the beam. Furthermore, enlarging the dimensionless maximum amplitude exhibits a similar effect on the post-buckling loads. Also, since CC boundary condition leads to higher stiffness, CC beams show greater values of post-buckling loads in comparison with SS beams.

By comparing the results obtained for UD and FG distributions in the case of beams with different boundary conditions in Fig. 3, it is found that at  $w_{max}=0$ , buckling load of UD beam is higher than that of FG beam, but by enhancing the  $w_{max}$ , the post-buckling loads of FG beam enhance faster than those of UD beam which is due to asymmetric distribution of CNTs in the matrix.

Post-buckling loads of the first three buckling modes for FG-CNTRC beams with  $V_*^{cnt}=0.12$  are presented in Fig. 4. It can be seen that for SS beams, by increasing the maximum deflection, the distance among the post-buckling load curves along the way enhances. However, the post-buckling loading curve of the second mode approaches to the third mode curve for the case of CC beams. Fig. 5 depicts the dimensionless post-buckling loads versus slenderness ratio for SS FG-CNTRC beams with different volume fractions at  $w_{max}=1$ . As it is observed, due to lower stiffness of the beam with higher slenderness ratio, an increase in the slenderness ratio results in reduction of post-buckling load.

Also, it can be deduced that for larger values of the slenderness ratio, the effect of slenderness

ratio on the post-buckling load decreases.

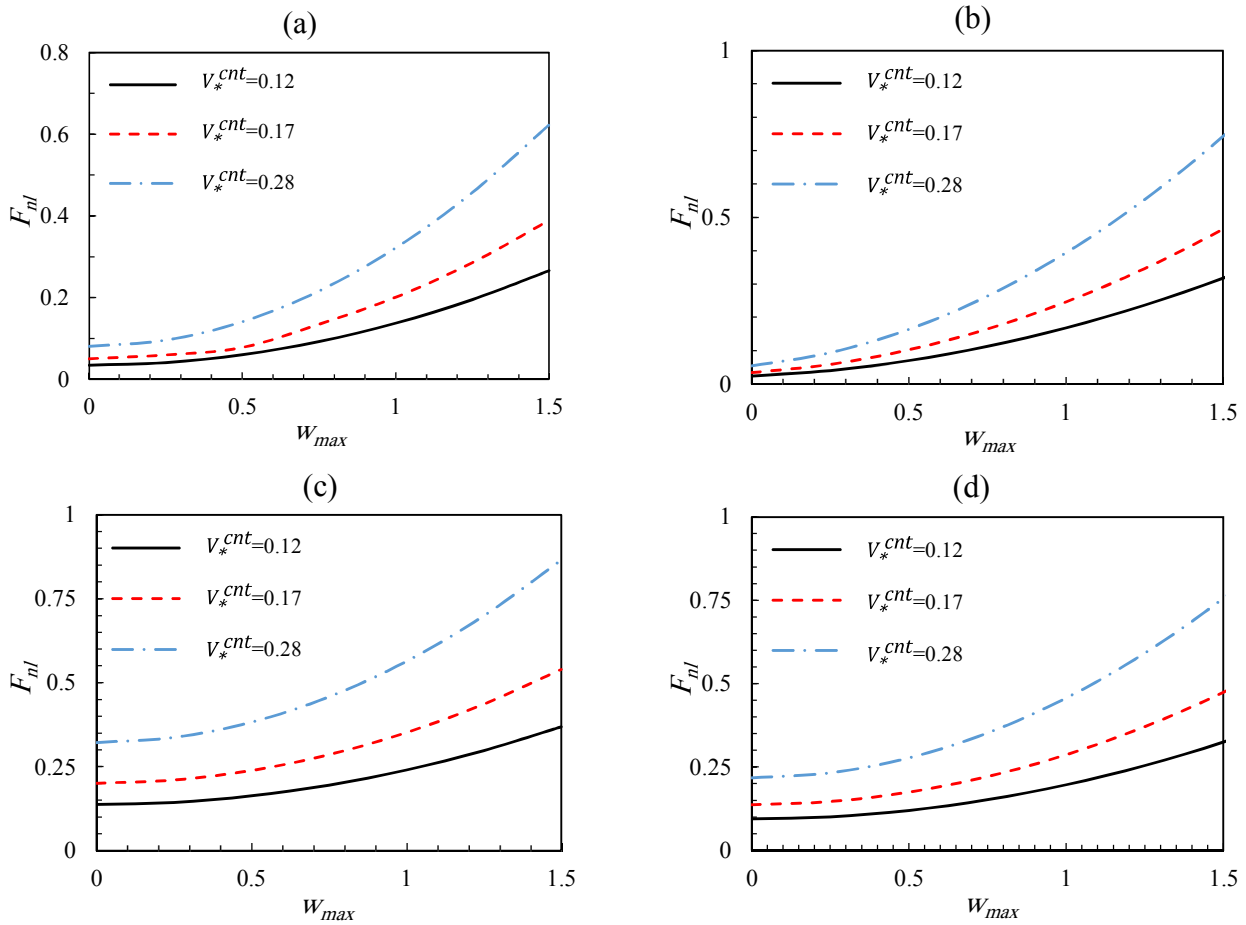


**Figure 3.** Dimensionless post-buckling loads for (a) SS UD-, (b) SS FG-, (c)CC UD-, and CC-FG CNTRC beams

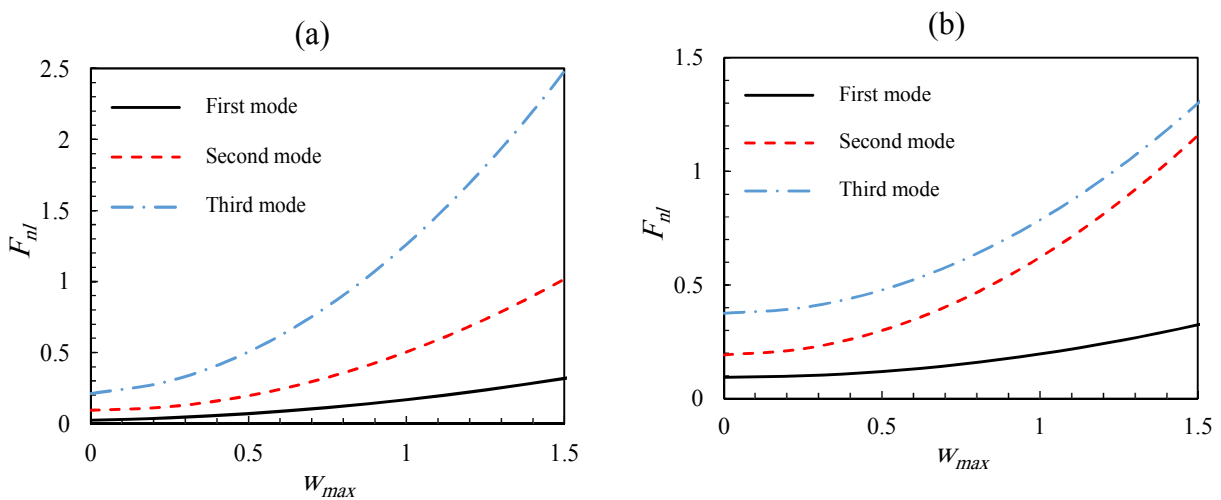


**Figure 4.** Dimensionless post-buckling loads of first three buckling modes for (a) SS, and (b) CC FG-CNTRC beams with  $V_*^{cnt} = 0.12$

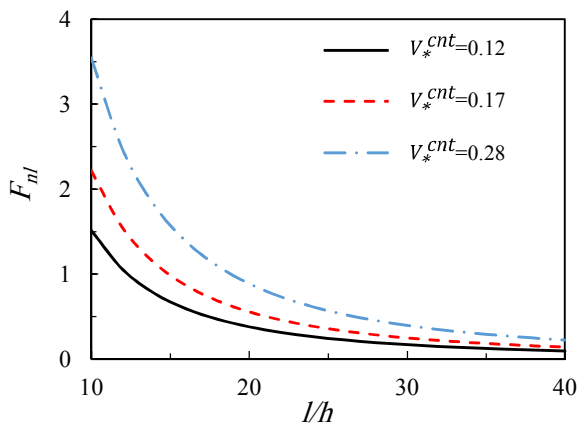


**Figure 5.** Dimensionless post-buckling loads versus slenderness ratio for SS FG-CNTRC beams

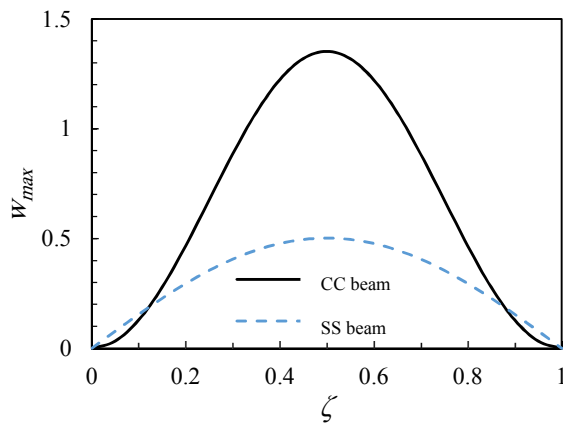


**Figure 6.** Buckling mode shapes of SS and CC FG-CNTRC beams with  $v_*^{cnt} = 0.12$

Fig. 6 plots the buckling mode shapes of SS and CC FG-CNTRC beams with  $v_*^{cnt} = 0.12$  subjected to buckling load ratio of  $F_{nl}/F_l=3$ . As expected, in the case of CC beams, the values of first derivatives with respect to  $\zeta$  at both ends of the beam are equal to zero. Moreover, due to higher stiffness of CC beams, their maximum deflection is greater than that of SS beams when the beams are subjected to the same buckling load ratios.

### Conclusion

This investigation presents the exact closed form solutions for post-buckling of CNTRC beams subjected to axial compressive loads. The extended rule of mixture is employed to predict the effective material properties of the nano-composite beam with UD and FG distributions of SWCNTs in the polymeric matrix. The material properties of FG beams are assumed to be graded in the thickness direction of the beam. Utilizing Euler-Bernoulli

beam theory together with the principle of virtual work, the governing equation of the nano-composite beam is derived. Moreover, the geometric nonlinear theory is modeled by applying von Kármán assumptions. An exact general solution with unknown constants is considered for the buckled configuration of the CNTRC beam and a characteristic equation is developed and solved to find the unknown constants as well as the corresponding characteristic values. The developed methodology is capable of carrying out parametric studies to analyze the influences of CNTs volume fraction, dimensionless maximum amplitude, slenderness ratio, distribution patterns and boundary conditions on the post-buckling behavior of the CNTRC beams. It is revealed from the results that increasing the CNTs volume fraction and dimensionless maximum deflection of the nano-composite beams enhances the dimensionless post-buckling loads. It is also found that increasing the slenderness ratio results in decreasing the post-buckling loads. Furthermore, the CC beams own higher post-buckling loads than SS beams.

### References

- [1] S. Iijima, "Helical microtubules of graphitic carbon", *Nature*, vol. 354, no. 6348, pp. 56-58, November 1991.
- [2] B.G. Demczyk, Y.M. Wang, J. Cumings, M. Hetman, W. Han, A. Zettl and R.O. Ritchie, "Direct mechanical measurement of the tensile strength and elastic modulus of multiwalled carbon nanotubes," *Materials Science and Engineering*, vol. 334, no. 1-2, pp. 173-178, September 2002.
- [3] H. Dai, "Carbon nanotubes: opportunities and challenges," *Surface Science*, vol. 500, no. 1-3, pp. 218-241, March 2002.
- [4] R. Ansari, H. Rouhi and S. Sahmani, "Free vibration analysis of single- and double-walled carbon nanotubes based on nonlocal elastic shell models," *Journal of Vibration and Control*, vol. 20, no. 5, pp. 670-678, April 2014.
- [5] H. Wan, F. Delale and L. Shen, "Effect of CNT length and CNT-matrix interphase in carbon nanotube (CNT) reinforced composites," *Mechanics Research Communications*, vol. 32, no. 5, pp. 481-489, September 2005.
- [6] Y. Han and J. Elliot, "Molecular dynamics simulations of the elastic properties of polymer/carbon nanotube composites: modeling

- and characterization,” *Computational Materials Science*, vol. 39, no. 2, pp. 315-323, April 2007.
- [7] E.T. Thostenson and T.W. Chou, “On the elastic properties of carbon nanotube-based composites: Modeling and characterization”, *Journal of Physics D: Applied Physics*, vol. 36, no. 5, pp. 573-582, February 2003.
- [8] V. Mittak, *Polymer nanotube nanocomposite: synthesis, properties and applications*, John Wiley and Sons, New Jersey, 2010.
- [9] A.M.K. Esawi and M.M. Farag, “Carbon nanotube reinforced composites: potential and current challenges,” *Materials and Design*, vol. 28, no. 9, pp. 2394-2401, November 2007.
- [10] K.M. Liew, Z.X. Lei and L.W. Zhang, “Mechanical analysis of functionally graded carbon nanotube reinforced composites: A review”, *Composite Structures*, vol. 120, pp. 90-97, February 2015.
- [11] B.S. Aragh, A.H.N. Barati and H. Hedayati, “Eshelby-Mori-Tanaka approach for vibrational behavior of continuously graded carbon nanotube-reinforced cylindrical panels”, *Composites Part B: Engineering*, vol. 43, no. 4, pp. 1943-1954, June 2012.
- [12] R. Ansari, M.F. Shojaei, V. Mohammadi, R. Gholami and F. Sadeghi, “Nonlinear forced vibration analysis of functionally graded carbon nanotube-reinforced composite Timoshenko beams”, *Composite Structures*, vol. 113, pp. 316-327, July 2014.
- [13] H. Shafiei and A.R. Setoodeh, “Nonlinear free vibration and post-buckling of FG-CNTRC beams on nonlinear foundation”, *Steel and Composite Structures*, vol. 24, no. 1, pp. 65-77, May 2017.
- [14] M. Shojaee, A.R. Setoodeh and P. Malekzadeh, “Vibration of functionally graded CNTs-reinforced skewed cylindrical panels using a transformed differential quadrature method”, *Acta Mechanica*, vol. 228, no. 7, pp. 2691-2711, July 2017.
- [15] D.G. Ninh, “Nonlinear thermal torsional post-buckling of carbon nanotube-reinforced composite cylindrical shell with piezoelectric actuator layers surrounded by elastic medium”, *Thin-Walled Structures*, vol. 123, pp. 528-538, February 2018.
- [16] L.L. Ke, J. Yang and S. Kitipornchai, “Nonlinear free vibration of functionally graded carbon nanotube-reinforced composite beams,” *Composite Structures*, vol. 92, no. 3, pp. 676-683, February 2010.
- [17] L.W. Zhang, Z.X. Lei and K.M. Liew, “Buckling analysis of FG-CNT reinforced composite thick skew plates using an element-free approach,” *Composite Part B: Engineering*, vol. 75, no. 15, pp. 36-46, June 2015.
- [18] A.R. Setoodeh and M. Shojaee, “Application of TW-DQ method to nonlinear free vibration analysis of FG carbon nanotube-reinforced composite quadrilateral plates,” *Thin-Walled Structures*, vol. 108, pp. 1-11, November 2016.
- [19] H.S. Shen, X.Q. He and D.Q. Yang, “Vibration of thermally postbuckled carbon nanotube-reinforced composite beams resting on elastic foundations”, *International Journal of Non-Linear Mechanics*, vol. 91, pp. 69-75, May 2017.
- [20] M.H. Yas and N. Samadi, “Free vibration and buckling analysis of carbon nanotube-reinforced composite Timoshenko beams on elastic foundation,” *International Journal of Pressure Vessels and Piping*, vol. 98, pp. 119-128, October 2012.
- [21] H.L. Wu, J. Yang, and S. Kitipornchai, 2016. “Imperfection sensitivity of postbuckling behavior of functionally graded carbon nanotube-reinforced composite beams,” *Thin-Walled Structures*, vol. 108, pp. 225-233, November 2016.
- [22] H.L. Wu, S. Kitipornchai and J. Yang, “Thermal buckling and postbuckling analysis of functionally graded carbon nanotube-reinforced composite beams,” *Applied Mechanics and Materials*, vol. 846, pp. 182-187, July 2016.
- [23] S. Poursmaeeli and S.A. Fazelzadeh, “Uncertain buckling and sensitivity analysis of functionally graded carbon nanotube-reinforced composite beam”, *International Journal of Applied Mechanics*, vol. 9, no. 5, pp. 1750071, July 2017.
- [24] S.A. Emam and A H. Nayfeh, “Postbuckling and free vibration of composite beams”, *Composite Structures*, vol. 88, no. 4, pp. 636-642, May 2009.
- [25] A.R. Setoodeh, M. khosrownejad and P. Malekzadeh, “Exact nonlocal solution for postbuckling of single-walled carbon nanotubes,” *Physica E*, vol. 43, no. 9, pp. 1730-1737, July 2011.

- [26] A. Fallah and M.M. Aghdam, "Nonlinear free vibration and post-buckling analysis of functionally graded beams on nonlinear elastic foundation," *European Journal of Mechanics A/Solids*, vol. 30, no. 4, pp. 571-583, July-August 2011.
- [27] R.K. Gupta, J.B. Gunda, G.R. Janardhan and G.V. Rao, "Post-buckling analysis of composite beams: Simple and accurate closed-form expressions," *Composite Structures*, vol. 92, no. 8, pp. 1947-1956, July 2010.